Phytochemistry 72 (2011) 2244–2252

Contents lists available at ScienceDirect

Phytochemistry

journal homepage: www.elsevier.com/locate/phytochem

Terpenoids and phenethyl glucosides from *Hyssopus cuspidatus* (Labiatae)

Megumi Furukawa [a], Mitsuko Makino [b], Emika Ohkoshi [a,1], Taketo Uchiyama [a], Yasuo Fujimoto [a,*]

[a] College of Pharmacy, Nihon University, 7-7-1 Narashinodai, Funabashi, Chiba 274-8555, Japan
[b] Department of General Education, College of Humanities and Sciences, Nihon University, 3-25-40 Sakurajousui, Setagaya, Tokyo 156-8550, Japan

ARTICLE INFO

Article history:
Received 14 March 2011
Received in revised form 15 June 2011
Accepted 8 July 2011
Available online 3 September 2011

Keywords:
Hyssopus cuspidatus
Labiatae
Abietane-type diterpenoids
Eremophilane-type sesquiterpenoid
Phenethyl glycosides
Leukotriene

ABSTRACT

Monoterpenoids (**3** and **4**), sesquiterpenoid (**2**), diterpenoid (**1**) and four phenethyl glucosides (**5**–**8**), together with fourteen known compounds, were isolated from the whole herb of *Hyssopus cuspidatus*. Their structures were determined by spectroscopic means. The abietane-type diterpenoids (**1**, **9**, **10**), rosmarinic acid (**15**) and salvigenin (**17**) inhibited leukotriene (LT) C_4 secretion from primary alveolar cells of Wistar rats.

1. Introduction

Hyssopus cuspidatus (Labiatae) is a folk medicine for treatment of fever and bronchus asthma in Xinjiang province, China. Although there are some reports on the constituents of this plant (Ablizl et al., 2009; Xue et al., 1990), those studies mainly focused on the essential oil of *H. cuspidatus*. In our biological studies on an alcohol extract of the whole herb of this plant, the extract was found to inhibit leukotriene (LT) C_4 secretion from primary alveolar cells of Wistar rats. In this paper, the isolation and structure elucidation are described of a new abietane-type diterpenoid (**1**), an eremophilane-type sesquiterpenoid (**2**), a pinane-type monoterpenoid (**3**), a menthane-type monoterpenoid (**4**) and four phenylethanoids (**5**–**8**) along with fourteen known compounds, 19, 20-epoxy-12-methoxy-11, 14, 19-trihydroxy-7-oxo-8, 11, 13-abietatriene (**9**) (Araújo et al., 2005), 11, 14-dihydroxy-12-methoxy-7-oxo-8, 11, 13-abietatrien-19–20β-olide (**10**) (Araújo et al., 2005), 10-hydroxycarvone (**11**) (Hamada et al., 1997), pinonic acid (**12**) (Fernández et al., 1993), loliolide (**13**) (Fernández et al., 1993), desacetylmatricarin (**14**) (Wong and Brown, 2002), rosmarinic acid (**15**) (Dapkevicius et al., 2002), coulterone (**16**) (Frontana et al., 1994), salvigenin (**17**) (Hòrie et al., 1998), genkwanin (**18**) (Hòrie et al., 1998), ursolic acid (**19**) (Tundisa et al., 2002), 2α-hydroxyursolic acid (**20**) (Murakami et al., 1993), 2α-hydroxyoleanolic acid (**21**) (Murakami et al., 1993), hyptadienic acid (**22**) (Taniguchi et al., 2002). The effect of the isolated compounds on the secretion of LTC_4 from primary alveolar cells of Wistar rats is also described.

2. Results and discussion

2.1. Structure elucidation

Compound **1** was obtained as a yellow amorphous powder. In the positive-ion HR EI-MS, a molecular ion peak at *m*/*z* 390.2035 (calcd 390.2042) $[M]^+$, was observed which is consistent with a molecular formula $C_{22}H_{30}O_6$. The ^1H NMR and ^1H–^1H correlation spectroscopy (COSY) spectra exhibited the presence of a tertiary methyl group [δ 0.97 (3H, s)], an isopropyl group [δ 1.38 (6H, d, J = 6.9 Hz), δ 3.31 (1H, sep, J = 6.9 Hz)], two methoxyl groups [δ 3.30, 3.78 (3H each, s)], a trimethylene (C-1–C-3) and a methine-methylene (C-5–C-6) sequences, and two hydroxyl proton signals [δ 5.76, 12.0 (1H each, s)] which were exchanged by adding D_2O. (Fig. 2 and Table 1). Analysis of the ^{13}C and ^{13}C-^1H COSY spectra indicates the presence of carbonyl (δ 205.4), acetal [δ_H 4.28 (1H, s), δ_C 105.4], and oxymethylene [δ 3.94 (1H, dd, J = 11.7, 2.1 Hz), δ 4.36 (1H, d, J = 11.7 Hz), δ_C 59.6] groups as well as benzene ring (δ 113.2, 127.0, 128.3, 139.8, 152.0, 157.0). The substitution pattern of the benzene ring was investigated by analysis of the heteronuclear multiple bond correlation (HMBC) spectrum of **1**. The methine proton signal (δ 3.31) of the isopropyl group exhibited the long-range correlations with the carbon resonances at δ

* Corresponding author. Present address: Department of General Education, College of Humanities and Sciences, Nihon University, 3-25-40 Sakurajousui, Setagaya, Tokyo 156-8550, Japan. Tel.: +81 3 5317 9365; fax: +81 3 5317 9433.
E-mail address: fujim-y@chs.nihon-u.ac.jp (Y. Fujimoto).
[1] Present address: Natural Products Research Laboratories, Eshelman School of Pharmacy, University of North Carolina, Chapel Hill, NC 27599, United States.

0031-9422/$ - see front matter © 2011 Elsevier Ltd. All rights reserved.
doi:10.1016/j.phytochem.2011.07.008

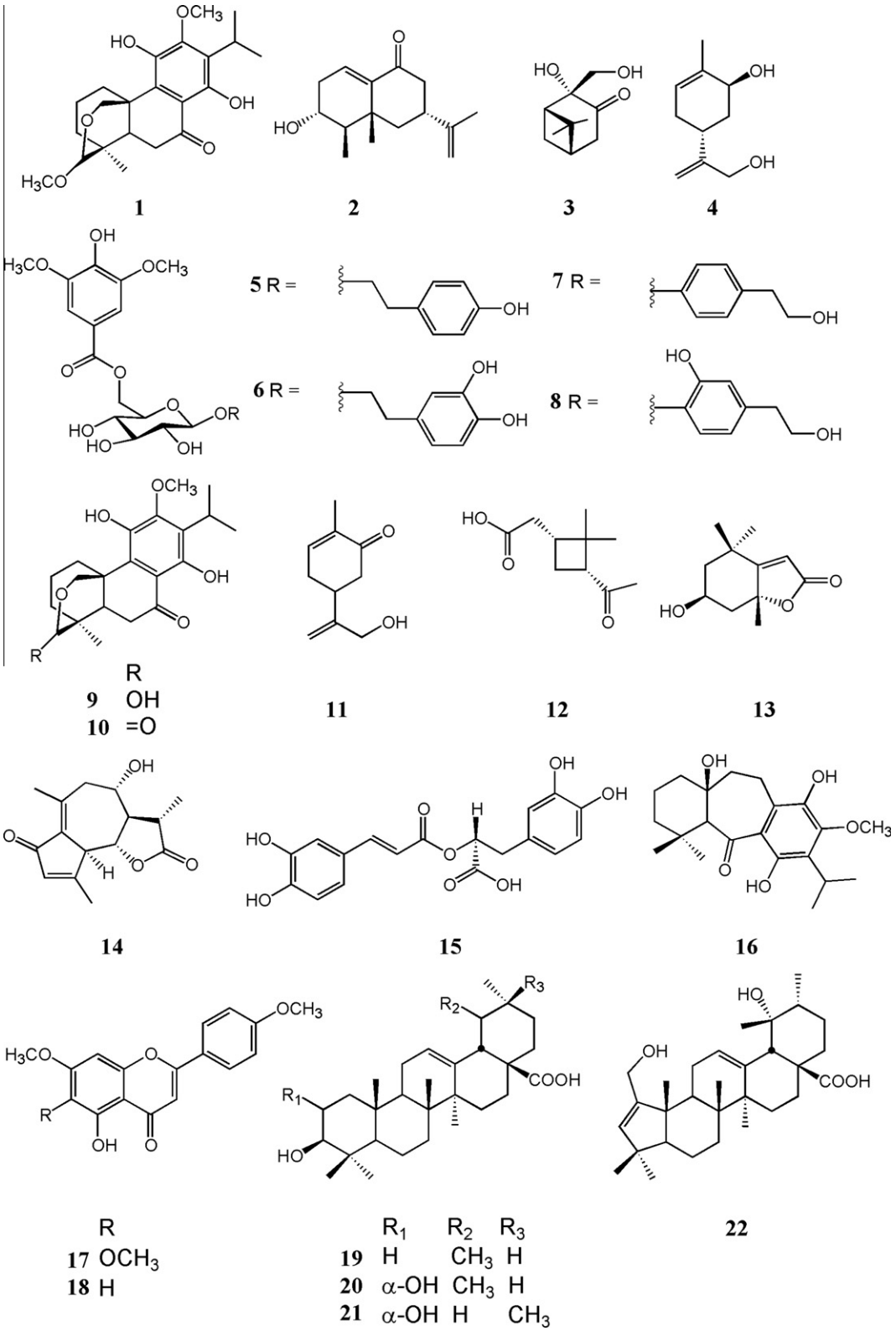

Fig. 1. Structures of Compounds **1**–**22**.

127.0 (C-13), δ 157.0 (C-14) and δ 152.0 (C-12) which have correlations with a methoxyl proton (δ 3.30) and as a hydroxyl proton (δ 5.76), signals suggesting the presence of a methoxyl group at C-12 and a hydroxyl group at C-11. The chemical shift value of the C-14 resonance (δ 157.0) and the low field shift of a hydroxyl proton signal (δ 12.0) indicated the presence of a hydrogen bonded-hydroxyl group at C-14 and the C-7 should be a carbonyl carbon (δ 205.4). This was further confirmed by the observation of long-range correlations between the hydroxyl proton (δ 12.0) and C-14 (δ 157.0) resonances besides the C-8 signal (δ 113.2). The connectivity of the other functional groups was also deduced by analysis of the HMBC spectrum. As shown in Fig. 2, long-range correlations were

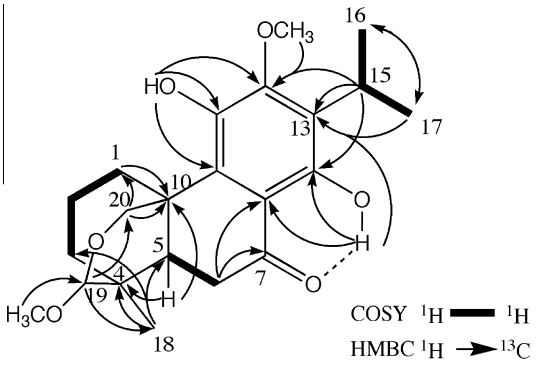

Fig. 2. Key HMBC Correlations for Compound **1**.

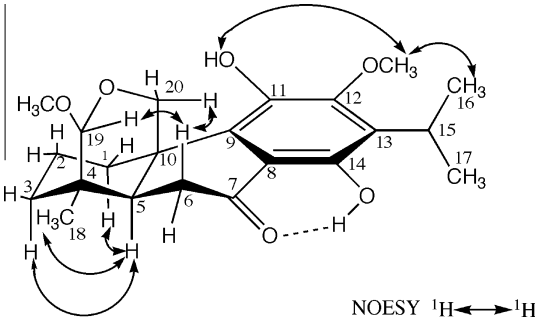

Fig. 3. NOESY Correlations for Compound **1**.

observed between the following proton and carbon signals: H-18 and C-3, C-4, C-5; H-19 and C-18, C-20; H-20 and C-1, C-10; H-5 and C-4, C-10; H-6 and C-7, C-8; *H*O-11 and C-9, C-11, C-12; H-15 and C-12, C-13, C-14; *H*O-14 and C-13, C-14, C-8. Thus, the structure of **1** was confirmed as shown in Fig. 2. The relative stereochemistry of **1** was assigned by analysis of the NOESY spectrum. The H-5 signal showed correlations with the H-1α, H-3α and H-18 signals, and the H-6β signal exhibited the correlations with H-19 and H-20 signals. Thus, the relative stereostructure of **1** was confirmed as shown in Fig. 3.

Compound **2** was obtained as a colorless oil. In the positive-ion HR EI-MS, a molecular ion peak at *m*/*z* 234.1616 (calcd 234.1620) $[M]^+$, consistent with a molecular formula $C_{15}H_{22}O_2$ was observed. The ^1H NMR spectrum of **2** showed the presence of a tertiary methyl [δ 0.98 (3H, s)], secondary methyl [δ 1.08 (3H, d, J = 6.5 Hz)], vinyl methyl [δ 1.76 (3H, brs)], oxymethine [δ 3.61 (1H, m)], and exomethylene [δ 4.76, 4.78 (1H each, brs)] groups and a vinyl proton [δ 6.45 (1H, s)] (Table 2). The ^{13}C NMR spectrum exhibited fifteen signals due to three methyl carbons (δ 11.5, 20.8, 26.1), an oxymethine carbon (δ 69.2), four sp^2 carbons (δ 110.7, 134.0, 145.3, 148.9), and a carbonyl carbon (δ 205.4) (Table 2). These spectroscopic data and the unsaturation degrees indicated that compound **2** should be a bicyclic sesquiterpene. Analysis of the ^1H-^1H COSY spectrum of **2** indicates the sequences of the C-1–C-15 through C-4 and the C-6–C-8 besides the presence of an isopropenyl group. The connectivity of these partial structures and the functional groups were investigated by analysis of HMBC spectrum. As shown in Fig. 4, the ^{13}C–^1H correlations due to the long-range coupling were observed between the following proton and carbon signals: H-1 and C-5, C-9, C-10; H-3 and C-4, C-5; H-15 and C-4, C-5; H-14 and C-4, C-5, C-6, C-10; H-12 and C-7, C-13, H-13 and C-7; H-7 and C-9; H-8 and C-9, suggesting the structure of **2** was as represented. Its relative stereochemistry was determined as shown in Fig. 4 by observation of the following NOESY correlations: H-15 and H-3, H-14; H-14 and H-7, H-6α and H-4, H-12. The absolute configuration of **2** was determined by application of new Mosher's method (Ohtani et al.,1991). The signals due to H-4, 14, and 15 of the (*S*)- α-methoxy-α-(trifluoromethyl) phenylacetyl (MTPA) ester of **2** appeared at higher fields than those of (*R*)-MTPA ester, while the H-1 signal of (*S*)-MTPA ester appeared at a lower field than that of (*R*)-MTPA ester, thereby indicating the stereochemistry at C-3 to be *R*-configuration. Thus, the absolute configuration of **2** could be assigned as 3*R*, 4*R*, 5*R*, 7*R* (Fig. 5).

Compound **3** was obtained as a pale yellow oil. In the positive-ion HR EI-MS, a molecular ion peak at *m*/*z* 184.1099 (calcd. 184.1099) $[M]^+$, which is consistent with a molecular formula $C_{10}H_{16}O_3$, was observed. Analysis of the ^1H and ^1H–^1H COSY spectra indicates the presence of a *geminal* dimethyl [δ 0.90, 1.38 (3H each, s)] and an oxymethylene [δ 3.37, 4.07 (1H each, d, J = 12.0 Hz)] group, and a sequence of CH-1–CH_2-7–CH-5–CH_2-4 (Table 2). The ^{13}C NMR spectra including DEPT showed 10 signals due to *geminal* dimethyl group [δ 22.6 (CH_3), 26.8 (CH_3), 39.3 (C), two methylene groups (δ 27.8 and 43.5), two methine groups (δ 38.1 and 46.7), an oxymethylene group (δ 67.7) and an oxygenated quaternary carbon (δ 77.1) and a carbonyl carbon (δ 216.2). These spectroscopic data suggested that compound **3** should be a bicyclic monoterpenoid. The connectivity of these partial structures and

Table 1
^1H and ^{13}C NMR Spectroscopic Data for Compound **1** (600 MHz, in $CDCl_3$).

Position	^1H (J, Hz)	^{13}C	Position	^1H (J, Hz)	^{13}C
1α	1.33 (1H, ddd, 13.8, 3.4, 2.1)	34.8	11		139.8
1β	3.42 (1H, dd, 13.8, 6.2)		12		152.0
2α	1.62[a]	21.7	13		127.0
2β	2.50 (1H, m)		14		157.0
3α	1.40 (1H, m)	39.5	15	3.31[b](1H, sep, 6.9)	26.1
3β	1.62[a]		16	1.38 (3H, d, 6.9)	20.3
4		36.4	17	1.38 (3H, d, 6.9)	20.3
5	1.88 (1H, dd, 15.8, 2.7)	44.3	18	0.97 (3H, s)	23.3
6α	3.27[b]	37.4	19	4.28 (1H, s)	105.4
6β	2.67 (1H, s, 15.8, 2.7)		20	3.94 (1H, dd, 11.7, 2.1)	59.6
7		205.4		4.36 (1H, d, 11.7)	
8		113.2	OCH_3	3.30 (3H, s)	54.8
9		128.3	OCH_3	3.78 (3H, s)	62.1
10		38.8	OH	5.76 (1H, s)	
			OH	12.0 (1H, s)	

The values in parentheses represent the coupling constants in Hz. The δ values are in ppm downfield from TMS.
[a] show overlapping of the signals.
[b] show overlapping of the signals.

Table 2
^{1}H- and ^{13}C-NMR Spectroscopic Data for Compound **2**–**4** (in $CDCl_3$).

	Compound **2**		Compound **3**		Compound **4**	
Position	^{1}H (*J*, Hz)	^{13}C	^{1}H (*J*, Hz)	^{13}C	^{1}H (*J*, Hz)	^{13}C
1	6.45 (1H, s)	134.0	2.07(1H, t, 6.1)	46.7		134.4
2	2.59 (1H, m) 2.14 (1H, m)	36.3		77.1	4.03 (1H, m)	68.5
3	3.61 (1H, m)	69.2		216.2	1.63 (1H, m) 1.96 (1H, m)	31.5
4	[a]1.57 (1H, m)	47.5	2.60 (2H, s)	43.5	2.43 (1H, m)	31.2
5		39.4	2.08 (1H, m)	38.1	2.18 (1H, m) 1.89 (1H, m)	37.0
6	2.00 (1H, m) [a]1.57 (1H, m)	43.0	2.60 (2H, s)	39.3	5.59 (1H, m)	125.2
7	2.36 (1H, m)	40.4	1.82 (1H,d, 11.0) 2.49 (1H, m)	27.8	1.81 (3H, br s)	20.8
8	2.34 (1H, m) 2.43 (1H, m)	44.1	0.90 (3H, s)	22.6		152.7
9		205.4	1.38 (3H, s)	26.8	4.92 (1H, br s) 5.09 (1H, br s)	108.7
10		145.3	3.37 (1H, d, 12.0) 4.07 (1H, d, 12.0)	67.7	4.16 (2H, m)	65.2
11		148.9				
12	1.76 (3H, br s)	20.8				
13	4.76 (s) 4.78 (s)	110.7				
14	0.98 (3H, s)	26.1				
15	1.08 (3H, d, 6.5)	11.5				

The values in parentheses represent the coupling constants in Hz. The δ values are in ppm downfield from TMS.
[a] shows overlapping of signals.

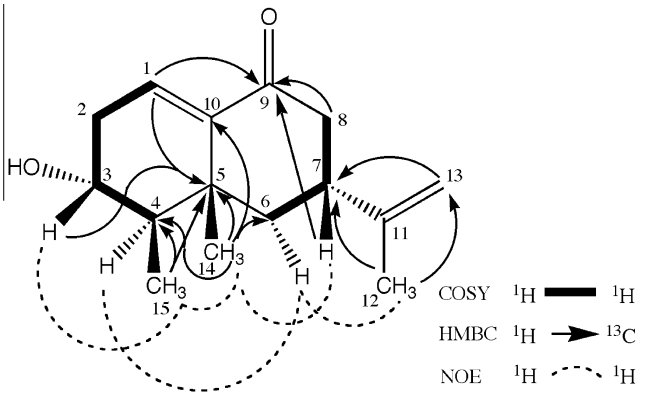

Fig. 4. Key HMBC and Difference NOE Correlations for Compound **2**.

functional groups were investigated by analysis of the ^{13}C–^{1}H long-range correlations. The HMBC spectrum of **3** exhibited cross-peaks between the following proton and carbon signals: H-10 and C-2, C-3; H-4 and C-3; H-8 and C-1, C-6; H-9 and C-5, C-6. In addition, the NOESY spectrum showed a correlation between H-8 and H-10 signals. Thus, the structure of **3** was defined as shown in Fig. 6.

Compound **4** was obtained as a colorless oil. In the positive-ion HR EI-MS, a molecular ion peak at *m*/*z* 168.1157 (calcd. 168.1150) $[M]^+$ was observed indicator of molecular formula $C_{10}H_{16}O_2$. The ^{1}H NMR spectrum showed the presence of vinyl methyl [δ 1.81 (3H, br s)], oxymethylene [δ 4.16 (2H, m)], oxymethine [δ 4.03 (1H, m)], and exomethylene [δ 4.92, 5.09 (1H each, br s)] groups, as well as a vinyl proton [δ 5.59 (1H, m)] (Table 2). Detailed analysis of ^{1}H–^{1}H COSY spectra suggested connectivity from C-2 to C-6 and C-9 to C-10 through C-8. Furthermore, the linkages between C-1 and C-2, and C-4 and C-8 were deduced by observation of the long-range correlations between following proton and carbon signals: H-7 and C-1, C-2, C-6; H-6 and C-1, C-2; H-2 and C-1; H-4 and

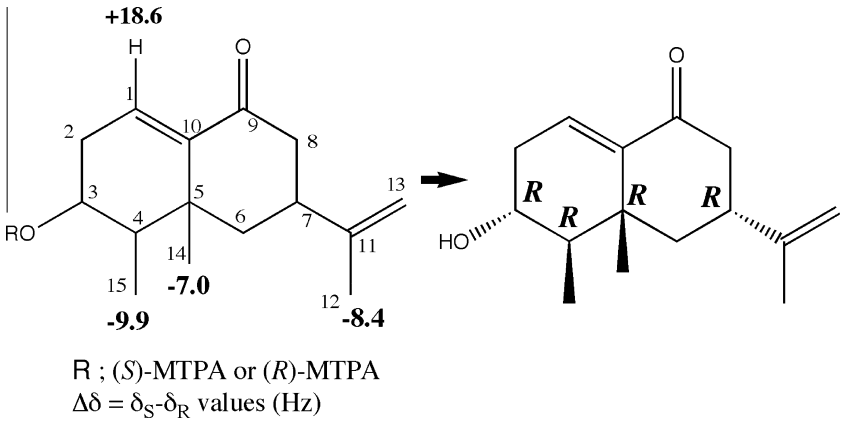

Fig. 5. Absolute Configuration for Compound **2**.

C-8; H-9 and C-4, C-10. The relative stereochemistry of **4** was determined by difference NOE experiments. Irradiation of the H-10 resonances at δ 4.16 produced a significant enhancement of the H-2 signal at δ 4.03. Thus, the relative stereostructure of **4** was confirmed as shown in Fig. 7. The absolute configuration of **4** was confirmed by application of the new Mosher's method. The resonance due to H-7 of the **4**-(*R*)-MTPA ester appeared at a higher field than that of **4**-(*S*)-MTPA ester, and H-3 and H-4 signals of **4**-(*R*)-MTPA ester appeared at lower fields than those of **4**-(*S*)-MTPA ester. Thus, the absolute configuration of **4** could be assigned as 2*S*, 4*R* (Fig. 8).

Compound **5** was obtained as a pale yellow oil. In the negative-ion HR FAB-MS, a quasi-molecular ion peak at *m*/*z* 479.1552 (calcd. 479.1553) $[M-H]^-$, consistent with a molecular formula $C_{23}H_{27}O_{11}$ was observed. The ^1H–^1H and ^{13}C–^1H COSY spectra indicated presence of a *p*-hydroxyphenethyl group [A] [δ 3.69 and 3.91 (1H each, m, H-1), δ 2.80 (2H, m, H-2), δ 6.65 (2H, d, J = 8.5 Hz, H-3′and H-5′), δ 6.95 (2H, d, J = 8.5 Hz, H-2′and H-6′)] and 3′,5′-*O*-dimethylgalloyl group [B] [δ 3.78 (6H, s, OCH_3 × 2), δ 7.32 (2H, br s, H-2‴and H-6‴), δ_c 168.0 (*C*OO) and a sugar moiety (see Tables 3 and 4)]. The connectivity of these partial structures was investigated by analysis of the HMBC spectrum. The H-1″ (anomeric proton) and the H-6″ signals of the sugar moiety exhibited cross-peaks with the carbon signals at δ 72.4 (C-1) and at δ 168.0 (COO), respectively, as well as the long-range correlations shown in Fig. 9. The sugar was identified as D-glucose by both TLC and gas chromatographic analysis of its trimethylsilyl thiazolidine derivative after alkaline and acid hydrolysis of **5** (see Experimental). Thus, structure **5** was confirmed as shown in Fig. 5.

Compound **6** was obtained as a pale yellow oil. In the negative-ion HR FAB-MS, a quasi-molecular ion peak at *m*/*z* 495.1500 (calcd. 495.1502) $[M-H]^-$, which is consistent with a molecular formula $C_{23}H_{27}O_{12}$ was observed. The ^1H and ^{13}C NMR spectra were very similar to those of **5** except for the presence of a 3,4-dihydroxyphenethyl group [δ 3.53 (2H, m, H-1), δ 2.44 (2H, m, H-2), δ 6.92 (1H, d, J = 2.0 Hz, H-2′), δ 6.74 (1H, d, J = 8.0 Hz, H-5′), and δ 6.75 (1H, dd, J = 2.0, 8.0 Hz, H-6′)] in place of the *p*-hydroxyphenethyl group. Thus, structure **6** was as shown in Fig. 1.

Compound **7** was obtained as a pale yellow oil. In negative-ion HR FAB-MS, a quasi-molecular ion peak at *m*/*z* 479.1554 (calcd 479.1553) $[M-H]^-$, which is consistent with a molecular formula $C_{23}H_{27}O_{11}$ was observed. The ^1H and ^{13}C NMR spectra of **7** showed close similarity to those of **5**. The HMBC spectrum of **7** exhibited a cross-peak between the anomeric proton signal (δ 4.84) and an oxygenated aromatic carbon resonance (δ 157.4, C-4′), suggesting the glycosidic linkage with a phenolic hydroxy group. Thus, the structure of **7** was represented as shown in Fig. 1.

Compound **8** was obtained as a pale yellow oil. In the negative-ion HR FAB-MS, a quasi-molecular ion peak at *m*/*z* 495.1496 (calcd. 495.1502) $[M-H]^-$, indicative of molecular formula $C_{23}H_{27}O_{12}$. The ^1H and ^{13}C NMR spectra were similar to those of **7** except for the presence of 1,2,4-trisubstituted benzene ring [δ 6.91 (1H, d, J = 2.0 Hz, H-3′), δ 6.74 (1H, dd, J = 2.0, 8.0 Hz, H-6′), δ 6.74 (1H, d, J = 8.0 Hz, H-5′)] in place of 1,4-disubstituted benzene ring. Thus, structure **8** was as shown in Fig. 1.

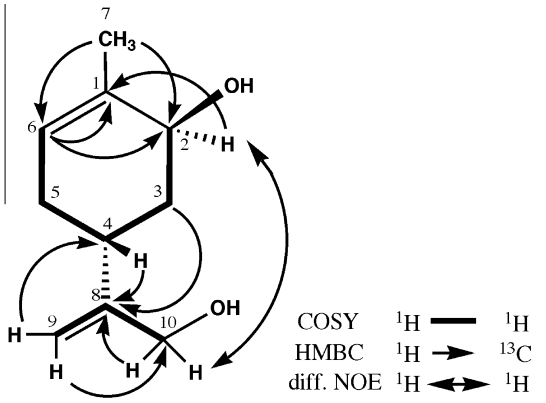

Fig. 7. Key HMBC and Difference NOE Correlations for Compound **4**.

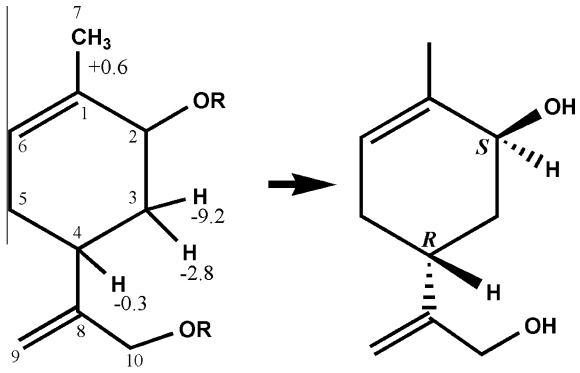

R ; (*S*)-MTPA or (*R*)-MTPA
$\Delta\delta = \delta_S - \delta_R$ values (Hz)

Fig. 8. Absolute Configuration for Compound **4**.

2.2. Assay

Metabolites of arachidonate such as LTC_4, LTD_4 and LTB_4, that are released from mast cells by an allergic reaction and from

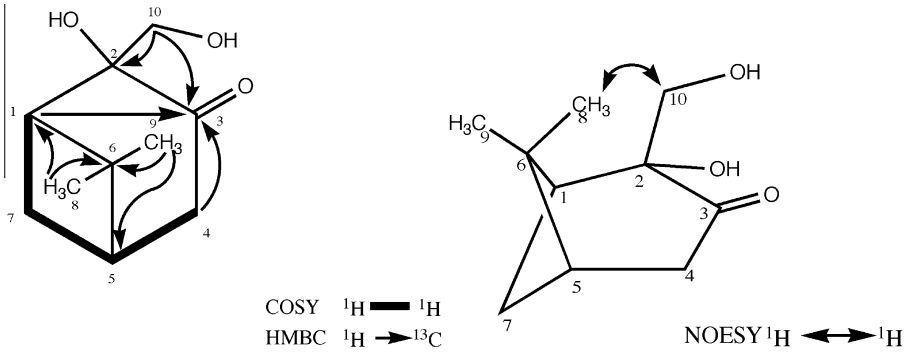

Fig. 6. Key HMBC and NOESY Correlations for Compound **3**.

Table 3
^{1}H-NMR Spectroscopic Data for Compound **5**–**8** (in MeOH-d_4).

^{1}H	Compound **5**	Compound **6**	Compound **7**	Compound **8**
Aglycone				
1	3.69–3.91 (2H, m)	3.53 (2H, m)	3.65 (2H, t, 7.1)	3.51 (2H, m)
2	2.80 (2H, m)	2.44 (2H, m)	2.69 (2H, t, 7.1)	2.74 (2H, m)
2′	6.95 (d, 8.5)	6.92 (d, 2.0)	6.93 (s)	
3′	6.65 (d, 8.5)		6.93 (s)	6.91 (d, 2.0)
5′	6.65 (d, 8.5)	6.74 (d, 8.0)	6.93 (s)	6.74 (dd, 8.0, 2.0)
6′	6.95 (d, 8.5)	6.75 (dd, 8.0, 2.0)	6.93 (s)	6.74 (d, 8.0)
Glucose				
1″	4.35 (d, 8.0)	4.77 (d, 7.8)	4.84 (d, 7.3)	4.77 (d, 6.1)
2″	3.22 (t, 8.0)	3.34–3.70 (4H, m)	3.35–3.56 (4H, m)	3.45–3.56 (4H, m)
3″	3.34–3.42 (2H, m)			
4″				
5″	3.62 (m)			
6″	4.38 (dd, 11.7, 6.8)	4.43 (dd, 12.0, 6.0)	4.42 (dd, 12.0, 7.8)	4.48 (dd, 11.9, 6.7)
	4.67 (dd, 11.7, 2.2)	4.72 (dd, 12.0, 2.2)	4.71 (dd, 12.0, 2.2)	4.72 (dd, 11.9, 2.1)
Galloyl				
2‴, 6‴	7.32 (2H, br s)	7.34 (2H, br s)	7.34 (2H, br s)	7.34 (2H, br s)
OCH_3	3.78 (6H, s)	3.86 (6H, s)	3.85 (6H, s)	3.86 (6H, s)

The Spectroscopic data for **5**–**7** were measured at 400 MHz and those for **8** were taken at 500 MHz.

Table 4
^{13}C NMR Spectroscopic Data for Compound **5**–**8** (in MeOH-d_4).

^{13}C	5	6	7	8	^{13}C	5	6	7	8
Aglycone					Galloyl				
1	72.4	70.1	64.2	64.1	1‴	121.2	121.2	121.3	121.2
2	36.5	36.3	39.4	39.2	2‴, 6‴	108.3	108.5	108.6	108.5
1’	130.5	132.2	157.4	132.1	3‴, 5‴	150.0	148.9	149.0	148.9
2’	130.8	119.9	117.8	119.9	4‴	142.3	142.2	142.3	142.2
3’	116.1	146.4	130.7	146.3	OCH_3	56.8	57.0	57.0	57.0
4’	156.8	146.9	157.4	146.8	COO	168.0	167.9	167.8	167.9
5’	116.1	118.0	130.7	117.0					
6’	130.8	125.8	117.8	125.5					
Glucose									
1”	104.6	104.5	102.5	104.5					
2”	75.1	75.8	75.5	75.8					
3”	78.0	77.4	77.9	77.4					
4”	72.2	71.9	72.2	71.9					
5”	75.4	74.8	74.9	74.8					
6”	65.3	65.1	65.2	65.1					

The Spectroscopic data for **5**–**7** were measured at 100 MHz and those for **8** were taken at 125 MHz.

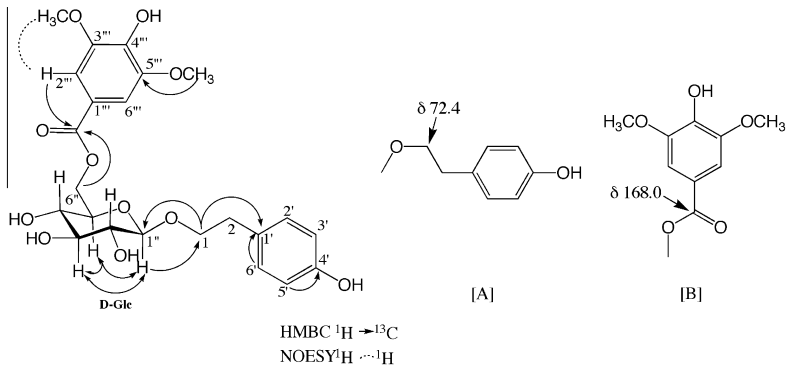

Fig. 9. Key HMBC and NOESY Correlations for Compound **5**.

eosinophils by inflammatory stimulations, are important in the pathogenesis of bronchial asthma. LTC_4 and LTD_4 constrict bronchial smooth muscle, stimulate mucus secretion from bronchial glands, and increase the permeability of airway vasculature. So the inhibition of LTC_4 secretion from primary alveolar cells of Wistar rats was next investigated. As shown in Table 5, among the isolated compounds, the abietane-type diterpenoids (**1**, **9**, **10**), rosmarinic acid (**15**) and salvigenin (**17**) showed inhibition of LTC_4 secretion to a similar extent or more potently than the ketotifen used as a positive control (Table 5). These results suggest that the phenolic

Table 5
Inhibitory Effects of Isolated Compounds on Release of LTC4.

Compounds	IC50 (μM)	Compounds	IC50 (μM)
1	42.9	12	>100
2	>100	13	>100
3	>100	14	92.5
4	>100	15	13.6
5	>100	16	-[a]
6	>100	17	39.9
7	>100	18	76.0
8	>100	19	-[b]
9	39.9	20	-[b]
10	23.3	21	-[b]
11	>100	Ketotifen	46.8

[a] not done.
[b] Compounds (**19**, **20** and **21**) exhibit cytotoxicity at the concentration of >10 μM.

compounds (**1**, **9**, **10** and **15**) having 1,4- or 1,2-dihydroxybenzene moieties and flavones (**17** and **18**) exhibit potent inhibition of release of LTC_4.

2.3. Conclusions

The constituents of *H. cuspidatus* have been investigated by several Chinese research groups (Ablizl et al., 2009; Xue et al., 1990). However, those studies have mainly focused on the essential oil of this plant. In the present studies, two monoterpenoids (**3** and **4**), a sesquiterpenoid (**2**), a diterpenoid (**1**) and four phenethyl glucosides (**5**–**8**), together with fourteen known compounds, were isolated from the whole herb of *H. cuspidatus*. The effect of the isolated compounds on the secretion of LTC_4 from primary alveolar cells of Wistar ratss is also investigated. The phenolic compounds (**1**, **9**, **10** and **15**) having 1,4- or 1,2-dihydroxybenzene moieties and flavones (**17** and **18**) potently inhibited release of LTC_4 from primary alveolar cells of Wistar rats.

3. Experimental

3.1. General

^1H and ^{13}C NMR spectra were measured on a JEOL JNM lambda-400, 500 spectrometer or JEOL ECA-600 in $CDCl_3$ or MeOH-d_4 containing TMS as an internal standard, with MS spectra being recorded on a HITACHI M-2000 instrument. IR spectra were acquired on a JASCO IR A-2. Column chromatography (cc) was carried out on silica gel (Wakogel C-200) and Diaion HP-20 (Nippon Rensui). HPLC was conducted with a Spectra Physics SP 8800 and Sensyu SSC-3160 pump equipped with either ERC-7520 (ERMA)-RI or HITACHI L-400-UV detector. Silica gel 60 F_{254} (Merck) precoated TLC plates were used and the detection was carried out by spraying 5% H_2SO_4 solution followed by heating.

3.2. Plant material

H. cuspidatus was collected in Xinjiang province, China and identified by Mr. Shen Jin Gui, Institute of Materia Medica, Shanghai Institutes for Biological Sciences, Chinese Academy of Sciences. A voucher specimen has been deposited in the above Institute and the Laboratory of Medicinal Chemistry, College of Pharmacy, Nihon University. (voucher No. HC-001, Laboratory of Medicinal Chemistry).

3.3. Extraction and isolation

Dried whole herb of *H. cuspidatus* (1.5 kg) was extracted with EtOH of (6.0 l × 4) under ultrasonication for each 30 min at 20–30 °C. The combine ethanol extract was concentrated under reduced pressure to give an oily material (81.6 g) which was applied to a Diaion HP-20 resin column, and then eluted successively with MeOH–H_2O (4:6, Fr. A), (7:3, Fr. B), MeOH (Fr. C) and acetone (Fr. D). Each fraction was concentrated *in vacuo* to give Fr.A (22.5 g), Fr.B (5.4 g), Fr.C (28.9 g), and Fr.D (18.9 g). Only Fr.B and Fr.C showed inhibitory activity on secretion of LTC_4 at a concentration of 100 μg/ml, in the bio-assay guided fractionation Fr. C was triturated with MeOH and the insoluble material was collected and recrystallized from EtOAc to give **19** (6100 mg). The mother liquor was concentrated to leave an oily material which was subjected to silica gel CC, this being eluted successively with hexane–EtOAc (5:1, 3.6 l, Fr. C-1–C-3), (3:1, 2.0 l, Fr.C-4), (2:1, 1.0 l, Fr.C-5), (1:1, 2.4 l, Fr.C-6), EtOAc (2.0 l, Fr.C-7) and MeOH (2.0 l, Fr.C-8) to give eight fractions. Fr. C-3 was fractionated by reversed phase HPLC {Kaseisorb LC PH SUPER, 20 × 250 mm (column A), MeOH–H_2O (75:25), flow rate 8 ml min^{-1}} to afford four fractions (Fr.C-3–1-C-3–4). Fr.C-3–3 was purified by reversed phase HPLC {Kaseisorb LC ODS PH SUPER, 10 × 250 mm (column B), MeOH–H_2O (9:1), flow rate 3 ml min^{-1}} to yield **16** (38 mg). Fr.C-4 was fractionated by reversed phase HPLC {column A, MeOH-H_2O (8:2), flow rate 8 ml min^{-1}} to afford four fractions (Fr. C-4–1–C-4–4). Fr.C-4–1 was further separated by reversed phase HPLC {column B, MeOH–H_2O (85:15), flow rate 3 ml min^{-1}} to give **1** (12 mg) and **10** (12 mg). Purification of Fr.C-4–2 using reversed phase HPLC {column B, MeOH–H_2O (85:15), flow rate 3 ml min^{-1}} to give **9** (75 mg). Separation of Fr. C-5 by reversed phase HPLC {column A, MeOH–H_2O (8:2), flow rate 8 ml min^{-1}} gave fourteen fractions (Fr.C-5–1–C-5–14). Purification of Fr. C-5–3 by reversed phase HPLC {column B, MeOH–H_2O (75:25), flow rate 3 ml min^{-1}} yielded **2** (15 mg). Fr. C-5–4 was purified by reversed phase HPLC {column B, MeOH–H_2O (75:25), flow rate 3 ml min^{-1}} to give **18** (4 mg). Compound **17** (7 mg) was obtained from Fr.C-5–6 by purification using reversed phase HPLC {column B (MeOH–H_2O (8:2), flow rate 3 ml min^{-1}}. Fr.C-5–10 was purified by reversed phase HPLC {Senshu Pak PEGASIL ODS, 10φ × 250 mm (column C), MeOH–H_2O (9:1), flow rate 3 ml min^{-1}} to give **22** (16 mg). Compounds **20** (47 mg) and **21** (29 mg) were obtained from Fr. C-5–12 and Fr. C-5–11, respectively, by purification using reversed phase HPLC {column C, MeOH-H_2O (9:1), flow rate 3 ml min^{-1}}. Fr. B (5.4 g) was subjected to silica gel CC, this being eluted, successively with $CHCl_3$–MeOH–H_2O {100:1:0 (300 ml, Fr. B-1), 10:1:0.05 (1650 ml, Fr. B-2), 8:2:0.2 (2500 ml, Fr. B-3), 7:3:0.3 (1000 ml, Fr. B-4, B-5), 6:4:0.5 (1000 ml, Fr. B-6), 6:4:1 (2000 ml, Fr. B-7) and acetone (Fr. B-8)} to give eight fractions. Fr.B-1 was further fractionated by silica gel CC {toluene–acetone 20:1 (500 ml, Fr.B-1–1), 10:1 (550 ml, Fr.B-1–2), 5:1 (1020 ml, Fr.B-1–3), 3:1 (600 ml, Fr.B-1–4), 2:1 (600 ml), 1:1 (600 ml), acetone (800 ml) Fr.B-1–5, MeOH (1000 ml, Fr.B-1–6)} to yield six fractions. Separation of Fr.B-1–4 by reversed phase HPLC {column A, MeOH–H_2O (4:6), flow rate 3 ml min^{-1}} afforded twelve fractions (Fr.B-1–4-1-B-1–4-12). Concentration of Fr.B-1–4-5 gave **3** (37 mg). Further separation of Fr.B-1–4-6 by reversed phase HPLC {column B, CH_3CN–H_2O (3:7), flow rate 3 ml min^{-1}} gave **13** (7 mg). Fr.B-1–4-7 was further purified by reversed phase HPLC (column B, CH_3CN–H_2O (32:68), flow rate 3 ml min^{-1}) to give **11** (5 mg). Compound **12** (17 mg) was obtained from Fr. B-1–4-8 by purification using reversed phase HPLC {column B, CH_3CN–H_2O (3:7), flow rate 3 ml min^{-1}}. Separation of Fr.B-1–4-9 by reversed phase HPLC {column B, CH_3CN–H_2O (25:75), flow rate 3 ml min^{-1}} yielded **14** (9 mg). Fr.B-1–4-11 was further purified by reversed phase HPLC {column B, CH_3CN–H_2O (3:7), flow rate 3 ml min^{-1}} to give **4** (6 mg). Fr.B-3 was fractionated by reversed phase HPLC {CAPCELL PAK UG, 20φ × 250 mm (column D), MeOH–H_2O (45:55), flow rate 8 ml min^{-1}} to afford four fractions (Fr.B-3–1–B-3–4). Separation of Fr.B-3–2 by reversed phase HPLC {column A, CH_3CN–H_2O (15:85), flow rate 3 ml min^{-1}}

gave **7** (10 mg) and **8** (3 mg). Compounds **5** (50 mg) and **6** (30 mg) were obtained by separation of Fr. B-3–3 using reversed phase HPLC {column B, MeOH–H_2O (1:1), flow rate 3 ml min^{-1}}. Fr.B-5 was further fractionated by reversed phase HPLC {column A, MeOH–H_2O (4:6), flow rate 8 ml min^{-1}} to afford five fractions (Fr.B-5–1–B-5–5). Compound **15** (15 mg) was isolated from Fr.B-5–1 by purification using reversed phase HPLC {column B, CH_3CN–H_2O (1:9), flow rate 3 ml min^{-1}}.

3.4. Compound *1*

Yellow amorphous powder; HR-EI-MS $[M]^+$ *m/z* 390.2035 (calcd. 390.2042 for $C_{22}H_{30}O_6$); $[\alpha]_D$ +95.2 (MeOH, *c* 0.25); UV λ_{max} (MeOH) nm (ε): 216 (4900), 240 (3800), 277 (3600), 368 (2200); For ^1H and ^{13}C NMR spectroscopic data, see Table 1.

3.5. Compound *2*

Colorless oil; HR-EI-MS $[M]^+$ *m/z* 234.1616 (calcd. 234.1620 for $C_{15}H_{22}O_2$); $[\alpha]_D$ +21.5 (MeOH, *c* 1.0); UV λ_{max} (MeOH) nm (ε): 241 (3800): For ^1H and ^{13}C NMR spectroscopic data, see Table 2.

3.6. Compound *3*

Pale yellow oil; HR-EI-MS $[M]^+$ *m/z* 184.1099 (calcd. 184.1099 for $C_{10}H_{16}O_3$); $[\alpha]_D$ +21.5 (MeOH, *c* 2.0); For ^1H and ^{13}C NMR spectroscopic data, see Table 2.

3.7. Compound *4*

Colorless oil; HR-EI-MS $[M]^+$ *m/z* 168.1157 (calcd. 168.1150 for $C_{10}H_{16}O_2$); $[\alpha]_D$ −7.7 (MeOH, *c* 0.5); For ^1H and ^{13}C NMR spectroscopic data, see Table 2.

3.8. Compound *5*

Pale yellow oil; HR-FAB-MS $[M-H]^-$ *m/z* 479.1552 (calcd. 479.1553 for $C_{23}H_{27}O_{11}$); $[\alpha]_D$ −9.3 (MeOH, *c* 1.0); UV λ_{max} (MeOH) nm (ε): 220 (11100), 278 (7 1 0 0); For ^1H and ^{13}C NMR spectroscopic data, see Tables 3 and 4.

3.9. Compound *6*

Pale yellow oil; HR-FAB-MS $[M-H]^-$ *m/z* 495.1500 (calcd. 495.1502 for $C_{23}H_{27}O_{12}$); $[\alpha]_D$ −56.2 (MeOH, *c* 1.0); UV λ_{max} (MeOH) nm (ε): 278 (8000), 379 (7700); For ^1H and ^{13}C NMR spectroscopic data, see Tables 3 and 4.

3.10. Compound *7*

Pale yellow oil; HR-FAB-MS $[M-H]^-$ *m/z* 479.1554 (calcd. 479.1553 for $C_{23}H_{27}O_{11}$); $[\alpha]_D$ −38.1 (MeOH, *c* 1.4); UV λ_{max} (MeOH) nm (ε): 278 (8000), 379 (7700); For ^1H and ^{13}C NMR spectroscopic data, see Tables 3 and 4.

3.11. Compound *8*

Pale yellow oil; HR-FAB-MS $[M-H]^-$ *m/z* 495.1496 (calcd. 495.1502 for $C_{23}H_{27}O_{12}$); $[\alpha]_D$ −33.8 (MeOH, *c* 0.12); UV λ_{max} (MeOH) nm (ε): 278 (8000), 379 (7700); For ^1H and ^{13}C NMR spectroscopic data, see Tables 3 and 4.

3.12. (S)-(−)-MTPA Ester of *2* (I. Ohtani et al., 1991)

To a stirred solution of **2** (1 mg) in pyridine (2 drops) was added one drop (large excess) of (*R*)-(−)-MTPA–Cl and stirring was continued overnight at room temperature. The mixture was diluted with EtOAc (1 ml) and then washed successively with brine and H_2O, dried (Na_2SO_4) and then concentrated *in vacuo*. ^1H NMR (500 MHz): Hz 410.55 (H-15), 476.40 (H-14), 756.70 (H-4), 857.75 (H-12), 2417.20 (H-13), 3283.25 (H-1).

3.13. (R)-(+)-MTPA Ester of *2*

The reaction was carried out in the similar manner as above. ^1H NMR (500 MHz): Hz 420.40 (H-15), 483.40 (H-14), 759.60 (H-4), 866.10 (H-12), 2424.40 (H-13), 3264.70 (H-1).

3.14. (S)-(-)-MTPA Ester of *4*

The reaction was carried out in a similar manner as described in the preparation of MTPA ester of **2**. ^1H NMR (500 MHz): Hz 855.45 (H-7), 902.75 (H-3), 961.60 (H-5) 1021.70 (H-3), 1029.35 (H-5), 1160.20 (H-4), 2818.30 (H-6).

3.15. (R)-(+)-MTPA Ester of *4*

The reaction was carried out in the similar manner as above. ^1H NMR (500 MHz): Hz 854.85 (H-7), 911.90 (H-3), 959.15 (H-5) 1024.45 (H-3), 1029.05 (H-5), 1160.50 (H-4), 2818.30 (H-6).

3.16. Absolute configuration of sugar in compound *5*, *6*, *7* and *8* (Hara et al., 1987)

Each glycoside (1 mg) was dissolved in 2% NaOMe/MeOH (1 ml) at room temperature. After 1 h, the reaction mixture was neutralized by passing each through an ion-exchange resion (Amberlite IRA 400, H^+ form) column. These were then heated in 1 M HCl (2 ml) at 90 °C for 3 h. After cooling, each reaction mixture was neutralized by individually passing each through an ion-exchange resin (Amberlite IRA 400, OH^- form) column. Each filtrate was then transferred to a Sep-Pak C18 cartridge and eluted with H_2O and MeOH, and the H_2O eluated were individuals concentrated and the residued were treated with L-cysteine methyl ester hydrochloride (2 mg) in pyridine (0.25 ml) at 60 °C for 1 h. After the reaction, the solution was treated with TMS-HT (100 μl, hexamethyldisilazane and trimethylchlorosilamine in pyridine, TOKYO KASEI Co., Tokyo, Japan) at 40 °C for 10 min. The reaction mixture was then subjected to GLC analysis to identify the derivatives of D-glucose from **5**, **6**, **7** and **8**. GLC conditions: column, ULBON HR-1, 25 m × 0.25 mm (i.d.), 0.25 μm; detector, FID; injector temperature, 250 °C; detector temperature, 280 °C; column temperature, 250 °C for 0.5 min and then 1.5 °C/min up to 270 °C; He carrier, 24 cm/s; D-glucose t_R, 6.83 min, respectively.

3.17. Measurement of LTC_4 secretion (Suzuki et al., 2001)

Wistar rats (6–10 weeks, female) were euthanized by decapitation and the pulmonary cavities were opened. After severing the descending aorta, the blood in the lungs was cleared by perfusion through the right heart with PBS (5 ml) containing of heparin 50 U/ml until the lungs became whitish. Using an 18-gauge needle, the trachea was cannulated, and of heparin/PBS (1 ml) was slowly injected into the lungs and then withdrawn. This procedure was repeated 7–10 times, and a total of 5–8 ml of lavage fluid was collected.

To obtain alveolar cell populations, lungs were perfused with heparin solution as above. Thereafter, they were aseptically removed and cut into small pieces. The dissected tissue was incubated in Dullbecco's modified Eagle's MEM (D-MEM) containing 1% penicillin–streptomycin (Cellgro) and 10% FBS, and digested lungs were further disrupted by gently pushing the tissue through

a nylon screen. The single-cell suspension was then washed and centrifuged at 500*g*. Cells were washed and resuspended 2×10^5 cells/ml of D-MEM, and plated on a 24-well plate for 500 μl/well incubated at 37 °C for 2 h. These cells were washed with PBS, and incubated in D-MEM containing 20 mM Hepes, pH 7.4 (Hepes-D-MEM) and test sample at 37 °C for 30 min and the cells were stimulated with calcium ionophore A23187 in Hepes-D-MEM, and incubated at 37 °C for 30 min.

LTC_4 content in supernatants was determined by LTC_4 Enzyme immunoassay (EIA) kit (Cayman Chemical, Ann Arbor, MI) according to the manufacturer's protocol. A dose–response curve was plotted for each compound, and the concentration giving 50% inhibition (IC_{50}) was calculated.($n = 3$).

References

Ablizl, P., Cong, Y., Musa, M., Zhu, Y., Kasimu, R., 2009. Chemical composition of the essential oil of Hyssopus cuspidatus from Xinjiang, China. Chem. Nat. Comp. 45, 445, and references cited therein.

Araújo, E.C.C., Lima, M.A.S., Nunes, E.P., Silveira, E.R., 2005. Abietane diterpenes from *Hyptis platanifolia*. J. Braz. Chem. Soc. 16, 1336–1341.

Dapkevicius, A., van Beek, T.A., Lelyveld, G.P., van Veldhuizen, A., de Groot, A., Linssen, J.P.H., Venskutonis, R., 2002. Isolation and structural elucidation of radical scavengers from *Thymus vulgaris* leaves. J. Nat. Prod. 65, 892–896.

Fernández, I., Pedro, J.R., Vidal, R., 1993. Norisoprenoids from *Centaurea aspera* and C. *Salmantica*. Phytochemistry 34, 733–736.

Frontana, B., Cárdenas, J., Rodríguez-Hahn, L., 1994. Diterpenoids from *Salvia coulteri*. Phytochemistry 36, 739–741.

Hamada, H., Yasumune, H., Fuchikami, Y., Hirata, T., Sattler, I., Williams, H.J., Scott, A.I., 1997. Biotransformation of geraniol, nerol and (+)- and (−)-carvone by suspension cultured cells of *Catharanthus roseus*. Phytochemistry 44, 615–621.

Hara, S., Okabe, H., Mihashi, K., 1987. Gas–liquid chromatographic separation of aldoseenantiomers as trimethylsilyl ethers of methyl 2-(polyhydroxyalkyl)-thiazolidine-4(*R*)-carboxylates. Chem. Pharm. Bull. 35, 501–506.

Hòrie, T., Ohtsuru, Y., Shibata, K., Yamashita, K., Tsukayama, M., Kawamura, Y., 1998. ^{13}C NMR spectral assignment of the A-ring of polyoxygenated flavones. Phytochemistry 47, 865–874.

Murakami, C., Myoga, K., Kasai, R., Ohtani, K., Kurokawa, T., Ishibashi, S., Darit, F., Padolna, W.G., Yamasaki, K., 1993. Screening of plant constituents for the effect on glucose transporter activity in ehrlich Ascites tumor cells. Chem. Pharm. Bull. 41, 2129–2131.

Ohtani, I., Kusumi, T., Kashman, Y., Kakisawa, H., 1991. High-field FT NMR application of Mosher's method. The absolute configuration of marine terpenoids. J. Am. Chem. Soc. 113, 4092–4096.

Suzuki, Y., Yoshimura, T., Yamashita, K., Matsui, T., Yamaki, M., Shimizu, K., 2001. Exposure of RBL-2H3 mast cells to ag^+ induces cell degranulation and mediator release. Biochem. Biophys. Res. Commun. 283, 707–714.

Taniguchi, S., Imayoshi, Y., Kobayashi, E., Takamatsu, Y., Ito, H., Hatano, T., Sakagami, H., Tokuda, H., Nishino, H., Sugita, D., Shimura, S., Yoshida, T., 2002. Production of bioactive triterpenes by *Eriobotrya japonica* calli. Phytochemistry 59, 315–323.

Tundisa, R., Deguinb, B., Menichinia, F., Tillequin, F., 2002. Iridoids from *Putoria calabrica*. Biochem. System. Ecol. 30, 689–691.

Wong, H., Brown, G.D., 2002. Dimeric guaianolides and a fulvenoguaianolide from *Artemisia myriantha*. J. Nat. Prod. 65, 481–486.

Xue, D., Chen, N., Pan, X., Liu, Y., 1990. Chemical constituents of the essential oil of *Hyssopus cuspidatus* Boriss. Gaodeng Xuexiao Huaxue Xuebao 11, 90–92.